A late Holocene molecular hydrogen isotope record of the East Asian Summer Monsoon in Southwest Japan

Els E. van Soelen [a, *], Naohiko Ohkouchi [c], Hisami Suga [c], Jaap S. Sinninghe Damsté [a, b], Gert-Jan Reichart [a, d]

[a] Utrecht University, Faculty of Geosciences, Department of Earth Sciences, P.O. Box 80.021, 3508 TA, Utrecht, The Netherlands
[b] NIOZ Royal Netherlands Institute for Sea Research, Department of Marine Microbiology and Biogeochemistry, Utrecht University, P.O. Box 59, 1790 AB, Den Burg, Texel, The Netherlands
[c] Japan Agency for Marine-Earth Science and Technology (JAMSTEC), 2-15 Natsushima-cho, Yokosuka, 237-0061, Japan
[d] NIOZ Royal Netherlands Institute for Sea Research, Department of Ocean Systems, Utrecht University, P.O. Box 59, 1790 AB, Den Burg, Texel, The Netherlands

ARTICLE INFO

ABSTRACT

Precipitation in Japan is strongly affected by the East Asian monsoon system, resulting in wet summer conditions and relatively dry winter conditions. Few paleo-monsoon records exist from northeastern Asia, especially records showing decadal- to centennial-scale variability. Here we present a molecular hydrogen isotope (δD) record from Lake Kaiike, a small coastal lake in southwest Japan, to provide insight into monsoonal precipitation over the past two millennia. The δD record of friedelin, a terrestrial higher plant lipid, reveals three major shifts in precipitation: a decline from > -185‰ to < -190‰ at 1700 cal yr BP suggests a change to wetter conditions; values between -187.5‰ and -180‰ from 1480 to 800 cal yr BP indicate reduced precipitation; and a decline to below -195‰ after 800 cal yr BP reflects moist conditions during the Little Ice Age. These results highlight variability in the intensity of the East Asian Summer Monsoon occurring on decadal to centennial time scales. El Niño-like conditions are likely responsible for periods of high monsoon intensity, but comparison with other records in the region (northeast China and Japan) shows that contradicting patterns also exist, and so explaining these rainfall patterns is not straightforward.

Introduction

Precipitation in large parts of Asia is strongly influenced by monsoonal winds. Offshore winds during winter result in relatively cool and dry conditions on land, while summers are warm and wet due to the prevailing inland winds (Lau and Li, 1984; Wang and Lin, 2002). The Asian monsoon systems can be divided into two sub-systems based on their different water sources and wind directions: the Indian and East Asian monsoon (Yihui and Chan, 2005). The East Asian Summer Monsoon (EASM) affects the eastern part of Asia, starting in mid-May in the south over the Philippines and southern China and then traveling northwards reaching northern China, South Korea, and Japan between June and late July (Wang and Lin, 2002; Yihui and Chan, 2005).

Inter-annual variability in the intensity of the EASM is related to various factors, including sea-surface temperature (SST) (Chang et al., 2000), snow cover on the Tibetan Plateau (Yanai et al., 1992), and changes in atmospheric circulation such as the Arctic Oscillation (Gong and Ho, 2003). Variability in the intensity of the East Asian Summer Monsoon has also been associated with the El Niño Southern Oscillation (ENSO) (Wang et al., 2001; Wu and Wang, 2002). ENSO variability not only affects the intensity of the summer monsoon but also influences the number of tropical cyclones or typhoons that make landfall in certain areas. During El Niño events, typhoons tend to curve towards the north and make landfall in Japan and South Korea, rather than in China (Wang and Chan, 2002; Elsner and Liu, 2003).

Only a few paleo-precipitation reconstructions exist from northeastern Asia, including Japan, South Korea, and northern China. Such reconstructions are important because the climate of the area is highly dynamic, and small changes in the location of high and low pressure cells can strongly influence rainfall patterns.

---

* Corresponding author. Present address: Department of Geosciences, University of Oslo, P.O. Box 1047 Blindern, 0316, Oslo, Norway.
E-mail addresses: evansoelen@gmail.com, e.e.v.soelen@geo.uio.no (E.E. van Soelen).

Yamada et al. (2010) reconstructed monsoon intensity for the last two millennia in the northeast of Japan and found centennial-scale climate fluctuations that can possibly be linked with known warm and cold periods in China and Europe (e.g., the Little Ice Age). Longer precipitation records exist from northern China. Hong et al. (2001) reconstructed precipitation based on plant $\delta^{13}C$ values in northeastern China for the past 6000 yr, and found eight periods of severe drought that can be linked with global events. Wen et al. (2010) studied Holocene precipitation changes based on pollen data from a lake in northeastern China and also found several shifts in precipitation and temperature occurring during the past 11,000 yr.

Woodruff et al. (2009) studied sediments from two small coastal lakes (Lake Namakoike and Lake Kaiike) in the southwest of Japan, which exist of laminated organic mud interbedded with coarse-grained units with elevated Sr levels. Typhoon landfall events may cause breaches in the barrier that separates the lakes from the sea, allowing Sr-rich marine material to enter the lakes (Woodruff et al., 2009). Therefore, the Sr record was interpreted to represent typhoon landfall events, and Woodruff et al. (2009) found that periods of barrier breaching coincide with an increase in El Niño frequency thus showing the importance of ENSO variability on typhoon landfall events. Especially between 36,000 and 2500 cal yr BP, elevated Sr levels coincide with increased El Niño frequency (Woodruff et al., 2009).

By reconstructing past changes in precipitation in the same area, it is potentially possible to study paleo-monsoon intensity and link this with ENSO variability and typhoon activity. In particular, changes occurring on centennial or decadal time scales are of interest as long-term trends in ENSO variability operate on these time scales, while there is still is the potential for individual typhoon events to be recognized.

In this study we present biomarker lipid data from Lake Kaiike to reconstruct past environmental conditions and precipitation patterns for the past 2000 yr. The laminated sediments of Lake Kaiike (Woodruff et al., 2009) indicate low oxygen conditions during sedimentation and hence good preservation of organic matter, which makes the site ideal for the analysis of organic geochemical proxies. We reconstructed past changes in precipitation using hydrogen isotope ratios of terrestrial higher plant lipids. In the tropics and subtropics, lower δD values of precipitation are generally related to higher amounts of precipitation due to the so-called "amount effect" (Dansgaard, 1964). Leaf waxes are, under the right conditions, able to capture the hydrogen signature of precipitation (Sachse et al., 2006; Liu and Yang, 2008), although evapotranspiration and biosynthetic fractionation result in a substantial offset between lipid and rainwater δD values (Sachse et al., 2004, 2006, 2012). Thus, a hydrogen isotope record based on terrestrial plant waxes from Lake Kaiike sediments could potentially be used to reconstruct past changes in summer precipitation in Japan. Such changes can subsequently be linked to larger scale processes like the East Asian Summer Monsoon intensity and ENSO variability.

Setting

Lake Kaiike is a small coastal lake on the northern shore of Kamikoshiki Island in the south of Japan (Fig. 1). The lake has a maximum depth of about 12 m, a surface area of 0.15 km^2 and a small drainage basin of only three times the size of the lake itself (Matsuyama, 1977). The lake is separated from the sea by a long gravel bar and from the adjacent Lake Namakoike by a stone bank (Fig. 1). Limited water exchange occurs between the sea and Lake Kaiike due to seepage of saltwater through the gravel bar (Matsuyama, 1977), and between the two lakes through a narrow connection in the stone bank. Currently, the lake is permanently

stratified, with oligotrophic and oxic fresh surface waters and saline deeper waters (Matsuyama, 1977). Productivity in the water column is highest near the chemocline, at approximately 5 m water depth, by chemolithotrophic and photoautotrophic (sulfur) bacteria, such as purple sulfur bacteria, green sulfur bacteria, and cyanobacteria (Nakajima et al., 2003). Lake Kaiike has a characteristic temperature profile with highest values between 4 and 6 m depth, and lower temperatures in surface (0–4 m) and deeper (6–12 m) parts (Matsuyama, 1977; Yamaguchi et al., 2010). This unusual temperature profile has been explained by adsorption of heat by the microbial population near the chemocline (Yamaguchi et al., 2010) and trapping of heat due to a lack of water circulation (Matsuyama, 1977).

Materials and methods

Material

A 240-cm-long sediment core (KAI-L2-2) was collected from the deepest part of Lake Kaiike (Fig. 1) using a gravity corer system in 2001. The core was divided into sections and subsequently stored frozen. After thawing, core sections were split longitudinally and visually described. A total of 22 samples, each 1 cm wide, were collected at approximately 10-cm intervals. The sediment in Section 1 was unconsolidated, such that less material was available for analysis. Thus, the uppermost 7 cm of the core was analyzed as a single unit. Samples were subsequently freeze-dried and stored frozen until the analyses were conducted.

Chronology

Previously, Woodruff et al. (2009) established an age model for the sediments of Lake Kaiike in their work on a parallel core that was also collected from the deepest part of the lake. That core, with a total length of almost 4 m, spans the past 4000 yr. Woodruff et al's. (2009) core was correlated to our core using distinct marker beds consisting of lighter colored, bioturbated sediments. To validate the applicability of the age model from Woodruff et al. (2009) for our core, a bivalve recovered from a depth of 227 cm was ^{14}C dated. This age was converted into calibrated years before present (cal yr BP) using the marine calibration curve in the Calib 7.1 program (Stuiver et al., 2015) resulting in an age of 2196 cal yr BP. A marine origin for the bivalve was assumed because it likely lived in situ in the lake sediments, and bottom water in the lake derives from seawater (Matsuyama, 1977). The data were fitted with a second order polynomial model: age (yr BP) = $(8.0 \times 10^{-3} \times depth^2) + (7.5 \times depth) - 51.0$. Our core is shorter than the Woodruff et al. (2009) core, spanning the past 2000 yr.

Total carbon content

To remove carbonates, 7.5 ml of 1 M HCl was added to about 0.3 g of freeze-dried and homogenized sediments. After shaking for 4 h, the acid was removed and 7.5 ml of 1 M HCl was added, after which the samples were shaken for 12 h. After removal of the acid, the sediments were washed with demineralized water and subsequently dried. Total organic carbon (TOC) was determined on the carbonate free residue using a NCS analyzer (Fison Instrument NA1500). Weight percentages of organic carbon were calculated relative to total sediment weight before carbonate removal.

Biomarker extraction, identification and quantification

Between 3 and 10 g of freeze dried sediments were repeatedly (5×) extracted using a mixture of dichloromethane (DCM) and
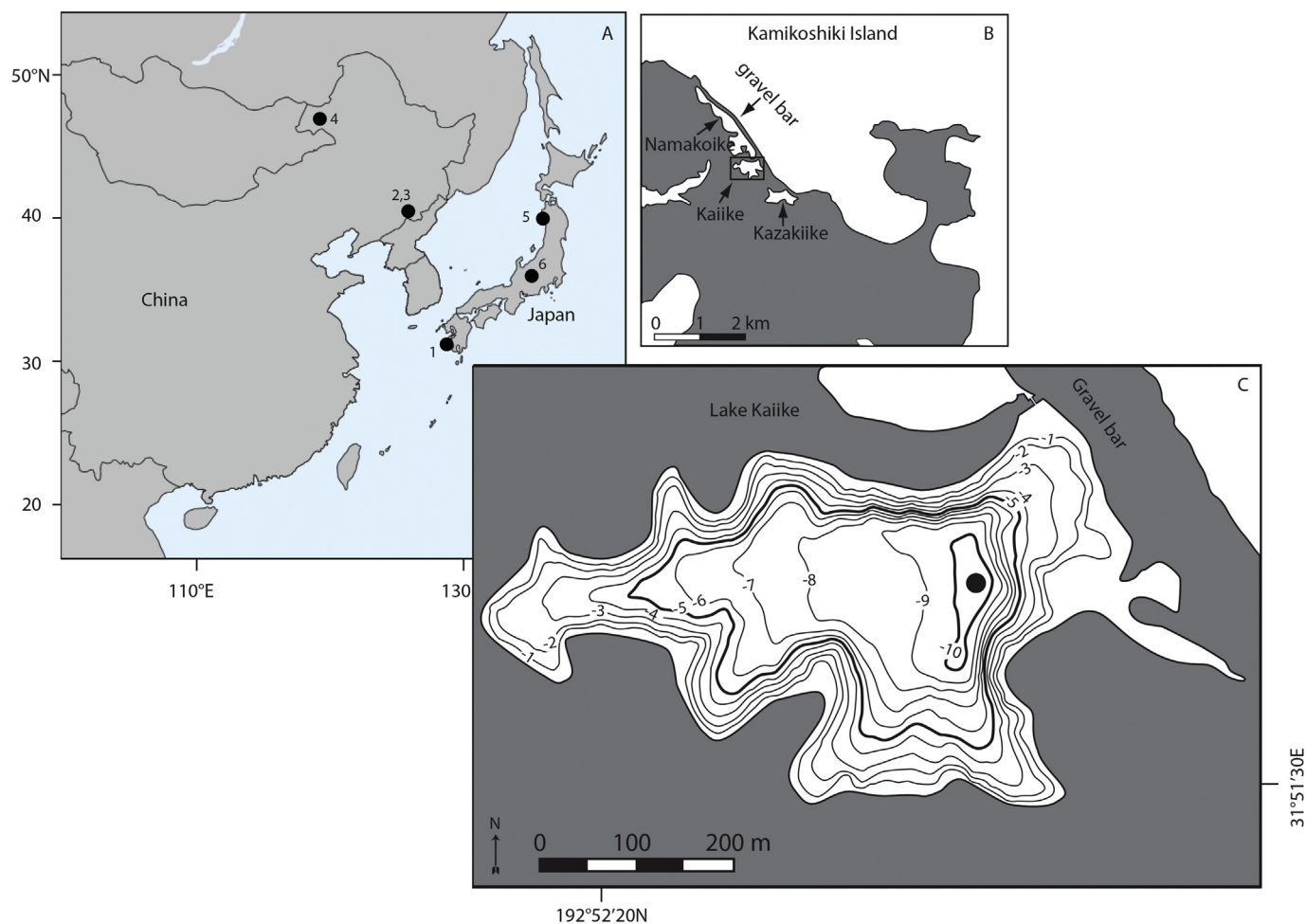
Figure 1. Maps showing: (A) the locations mentioned in this paper (Fig. 5), including 1 = Lake Kaiike and Lake Namakoike, 2 = Hani peatbog, 3 = Jinchuan peatbog, 4 = Hulun Lake, 5 = Lake San-no-megata, and 6 = Lake Aoki. (B) The location of Lake Kaiike and Lake Namakoike on Kamikoshiki Island. (C) Bathymetry of Lake Kaiike; black dot shows the core location, and contour intervals indicate depth in m. Figure adapted from Yamaguchi et al. (2010).

methanol (MeOH) (2:1) in an ultrasonic bath for 5 min. Extracts were combined and solvents were evaporated under a nitrogen stream until they were nearly dry. Elemental sulfur was removed using HCl-activated copper and traces of water were removed with a small $NaSO_4$ column. For analysis of "total lipids" (TLs), an aliquot of the extract was derivatized using diazomethane to convert fatty acids into methyl esters, after which the extracts were cleaned over a small silica column using ethyl acetate as an eluent. To derivatize alcohols into trimethylsilyl (TMS) ethers, 25 μl pyridine and 25 μl BSTFA (N,O-bis(trimethylsilyl) trifluoroacetamide) were added to approximately 2 mg of sample. The sample was then heated in an oven at 60°C for 20 min and subsequently dissolved in ethyl acetate. A known amount of the internal standard (squalane) was added to allow for quantification of the biomarkers. The remainder of the extract was separated into fractions with different polarity using a small Pasteur pipette filled with activated Al_2O_3 and eluted with 1) hexane, 2) DCM, and 3) DCM:MeOH (v/v 1:1), resulting in hydrocarbon, ketone, and polar fractions, respectively. Ketone fractions were further purified for compound-specific isotope analysis using a small (dimension approximately 5 mm × 4 cm) column packed with Ag^+-impregnated silica. Elution with DCM resulted in a fraction containing friedelin, while elution of the column with ethyl acetate resulted in a fraction containing unsaturated ketones.

TL and other fractions were analyzed by gas chromatography (GC) using an HP gas chromatograph fitted with a CP-Sil 5CB fused silica capillary column (30 m, 0.32 mm i.d.) and a flame ionization detector (FID). Samples were injected on-column, with helium as carrier gas set at constant pressure (100 kPa). The oven temperature increased from 70°C up to 130°C by heating with 20°C per min, then up to 320°C by heating with 4°C per min, and then kept at this temperature for 20 min. Mass spectrometry was performed using a GC−MS (ThermoFinnigan Trace GCMS) with the same type of column and oven program as used for the GC, but using constant flow of the carrier gas. Compounds were identified based on retention times and mass spectra.

Long chain n-alkanes, present in the hydrocarbon fractions, were used to calculate average chain length (ACL) and carbon preference index (CPI).

$$ACL = \frac{([C25]*25 + [C27]*27 + [C29]*29 + [C31]*31 + [C33]*33)}{([C25] + [C27] + [C29] + [C31] + [C33])}$$

(1)

$$CPI = 0.5*\left(\frac{([C25] + [C27] + [C29] + [C31] + [C33])}{([C24] + [C26] + [C28] + [C30] + [C32])}\right.$$
$$\left. + \frac{([C25] + [C27] + [C29] + [C31] + [C33])}{([C26] + [C28] + [C30] + [C32] + [C34])}\right)$$

(2)

Stable hydrogen isotopic composition of friedelin

Stable hydrogen isotope ratios of friedelin were measured on a GC-IRMS (Delta plus XP), by injection of the friedelin fraction using the same method and program as for the GC, but using a constant flow instead of constant pressure. The H_3^+ factor was determined every day and was always below 5.5. Schimmelmann Mixture A (a mixture of even numbered C_{16}–C_{30} *n*-alkanes with δD values of −42.7−256.4‰, purchased from A. Schimmelmann, Biogeochemical Laboratories, Indiana University) was run at the start of each sequence (and repeated during the day in case of long sequences) and used to calibrate the measured sample values against VSMOW. Squalane (also from Schimmelmann) with a known δD composition was co-injected as internal standard to monitor performance. Hydrogen isotope ratios (δD) were normalized to the VSMOW scale. Samples were measured at least in duplicate and only well resolved peaks with a high intensity (>500 mV) were integrated. The standard deviation per sample was always <3.5‰.

Results

Chronology

The available age controls (data from Woodruff et al., 2009), a ^{14}C-dated shell, and the core top were combined into one age model (Fig. 2). Sedimentation rates increase from 0.9 mm yr^{-1} near the base of the core, up to 1.3 mm yr^{-1} in the core top. ^{210}Pb analyses reported for surface sediment of lake Kaiike by Kotani et al. (2001) indicate still higher modern sedimentation rates of around 2.3 mm yr^{-1}. Sedimentation rates in the upper part of the core are likely higher because the sediments are unconsolidated, whereas the sediments become more and more compacted with prolonged burial.

TOC content

The total organic carbon (TOC) content varies between 1.8 and 8.5 wt% (Fig. 3A). Lower TOC content (<5%) was found in three intervals: >1970 cal yr BP, 1400−1000 cal yr BP, and 400−40 cal yr BP.
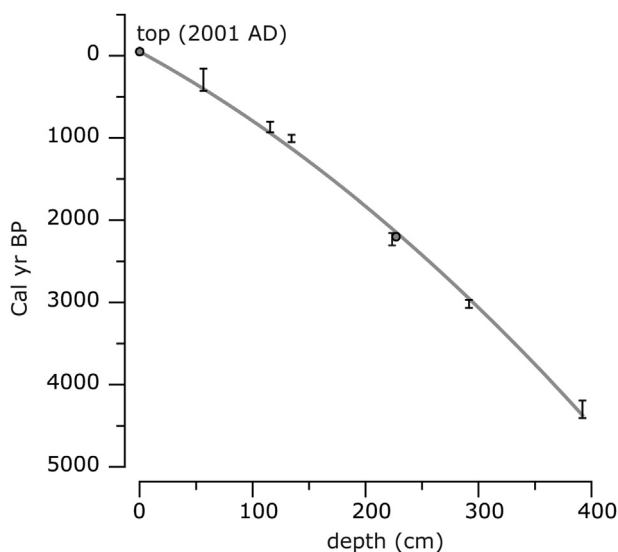

Figure 2. Age model for Lake Kaiike based on the combined data from Woodruff et al. (2009) (black error bars) and this study (gray dots).

Lipid biomarkers

Friedelin is an abundant lipid throughout the record, with concentrations generally ranging between 0.1 and 2.2 mg g^{-1} TOC (Fig. 3B). At ca. 1635 and 910 cal yr BP friedelin concentrations show peak values of 5.1 and 12.6 mg g^{-1} TOC, respectively. At ca. 1110 cal yr BP and at the top of the record, concentrations of friedelin were below the detection limit. The records of long-chain *n*-alkanes (C_{25}–C_{33}) (Fig. 3C) and *n*-alcohols (Fig. 3D) show comparable concentration patterns as friedelin, although absolute values are lower: maximum concentrations are 2.5 and 3 mg g^{-1} TOC for *n*-alkanes and *n*-alcohols, respectively. The ACL of *n*-alkanes in the Lake Kaiike sedimentary record varies between 29.3 and 30.3 (Fig. 3E), and the CPI varies between 3 and 9 (Fig. 3F). Both records show a trend towards lower values in recent sediments.

Concentrations of tetrahymanol reached as high as 4.5 mg g^{-1} TOC (Fig. 3G) but were low (<0.5 mg g^{-1} TOC) in sediments older than 1700 cal yr BP, between 1420 and 1100 cal yr BP, and around 40 cal yr BP. Dinosterol concentrations reached 1.8 mg g^{-1} TOC (Fig. 3H) and were low in the same intervals as noted for tetrahymanol. C_{37} and C_{38} alkenones were detected at relatively low concentrations (<0.1 mg g^{-1} TOC) in only a few sediment depths (2090, 1970, and 1310 cal yr BP) (Fig. 3I).

Hydrogen isotopes

The total range of the hydrogen isotope values of friedelin is ca. 25‰, with an average of −188‰ (Fig. 5A). Values are higher than average (−174.0 to −184.6‰) between 2090 and 1700 cal yr BP, lower than average (−190.9 to −192.6‰) between 1700 and 1480 cal yr BP, higher than average (−180.8 to −187.4‰) from 1480 to 800 cal yr BP, and again below average (195.5 to −198.8‰) from 800 cal yr BP onwards. In the uppermost sediments (i.e., the last 360 yr) friedelin concentrations were too low to obtain reliable δD values.

Discussion

Potential sources of biomarkers present in the lake record

The total organic carbon (TOC) content in the studied sediments varies between 2 and 8.5% (Fig. 3A), indicating excellent preservation of organic matter throughout the record. Long-chain *n*-alkanes and *n*-alcohols derive from the leaf waxes of higher plants (Eglinton and Hamilton, 1967). Dust, transported from arid regions in central Asia during the winter monsoon, could provide a potential source of these leaf waxes (Yokoyama et al., 2006). However, Lim et al. (2005) reconstructed dust transport in Northeast Asia for the past 6500 yr and found low eolian quartz fluxes for the past 2000 yr. Furthermore, centennial-scale fluctuations in the dust flux (Lim et al., 2005) show no correlation with the abundance pattern of terrestrial leaf waxes in the Lake Kaiike sediments (Fig. 3). Therefore, the input of wind-transported *n*-alkanes is likely negligible compared to the production by local vegetation. Chikaraishi et al. (2012) showed that long-chain *n*-alkanes are also abundant in various insects and organisms in the soil, with chain lengths comparable to plant-derived *n*-alkanes. Insects could, therefore, be a potential alternative source for *n*-alkanes in the Lake Kaiike sediments.

Pentacyclic triterpenoids, such as friedelin, are also common components of the leaves of terrestrial higher plants (Volkman, 2005). Friedelin has been detected in leaves, but also in bark and stem tissue of a variety of different terrestrial higher plants (Chandler and Hooper, 1979); it is not specific to certain plant families (Sainsbury, 1970). The high amounts of friedelin in the Lake
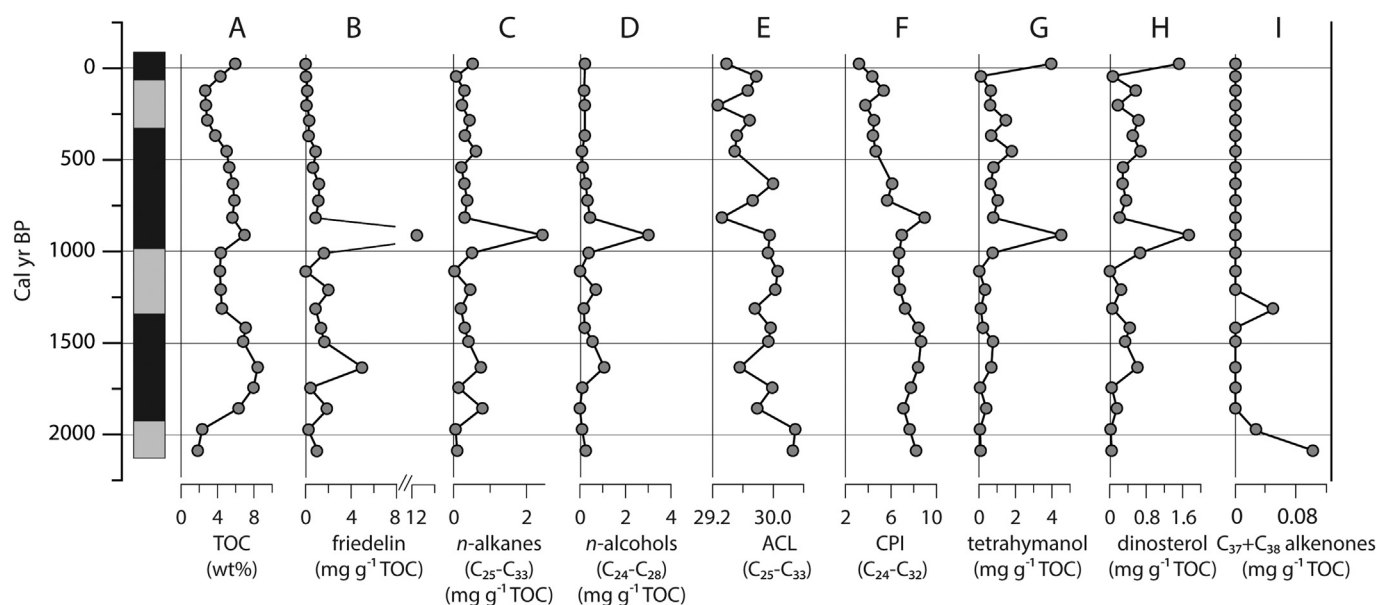
Figure 3. Organic geochemical data from the Lake Kaiike sediment core. A) Total organic carbon (TOC) content in wt%, B) friedelin concentration, C) n-alkanes concentration, D) n-alcohols concentration, E) ACL (average chain length) of n-alkanes, F) CPI = carbon preference index of n-alkanes, G) tetrahymanol concentration and H) dinosterol concentration and I) alkenone concentration. The lithological column (left) shows dark, laminated, and organic-rich intervals (black) and bioturbated intervals with lower TOC content (gray).
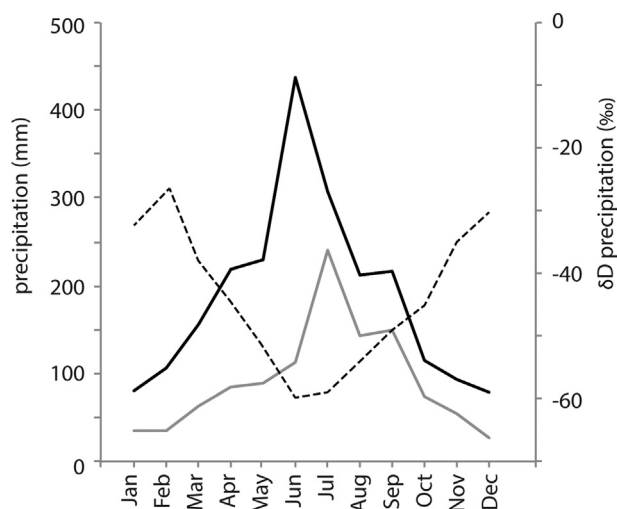

Figure 4. Monthly average precipitation (1961–1976) (gray line) and associated hydrogen isotope ratios (dashed line) for Pohang, South Korea (data from IAEA/WMO, The GNIP Database) and average monthly precipitation rates for Kagoshima, Japan (1883–2015) (black line) (Lawrimore et al., 2011).

Kaiike sediments, therefore, most likely derive from higher plants fringing the lake. Decreasing concentrations of friedelin at the top of the record may result from a change or reduction in vegetation cover surrounding the lake. A gradual trend towards lower CPI and ACL values during the past two millennia was observed (Fig. 3E, F). This pattern is likely also a local expression of vegetation change near Lake Kaiike, but it is not observed in any of the other proxies.

In addition to terrestrially derived lipids, lipids from aquatic sources were also detected in the sediments. Tetrahymanol is produced by ciliates (Sinninghe Damsté et al., 1995) and certain anaerobic eukaryotes (Takishita et al., 2012) in hypoxic environments and is, therefore, indicative of water column stratification. Dinosterol, which is produced by many dinoflagellate species (Alam et al., 1979; Boon et al., 1979) and in small amounts also by diatoms

(Volkman et al., 1993), was found throughout the sedimentary record (Fig. 3I). Low amounts of C_{37} and C_{38} alkenones were also detected within the intervals that represent ventilated conditions of the lake (see below). Alkenones are produced by Prymnesiophyceae (Marlowe et al., 1984), including open marine coccolithophore-species like *Emiliania huxleyi* and *Gephyrocapsa oceanica* (Volkman et al., 1980; Marlowe et al., 1990), and coastal haptophytes (Rontani et al., 2004). Alkenones are also known to occur in freshwater (Zink et al., 2001) and hypersaline environments (Lopez et al., 2005). The different depositional environments can be reflected in the relative distribution of the different types of alkenones. However, due to the low abundance of alkenones in the Lake Kaiike sediments, the various methyl and ethyl alkenones could not be distinguished.

Water column stratification and ventilation

The Lake Kaiike core shows several phases with sediments characterized by a lighter color, a lower TOC content, and indications for bioturbation (Fig. 3A; gray intervals). At present, Lake Kaiike experiences strong, year-round density stratification (Matsuyama, 1977) with a fresh surface-water layer and more saline deeper waters. Lower TOC contents in the past probably indicate that the water column was (at least periodically) ventilated. Indeed, tetrahymanol, an indicator for stratification of the water column (Sinninghe Damsté et al., 1995), shows low concentrations in sediments >1970 cal yr BP and in the period between 1310 and 1000 cal yr BP, thus supporting the inferred changes in water column ventilation. Alkenones were only detected in the intervals with a low TOC content. The environmental conditions that allowed for alkenone production in the lake thus seem related to the same episodes resulting in water-column ventilation. This interpretation is consistent with the alkenones being produced by marine coccolithophores, since water column mixing would result in higher surface water salinities. Irrespective of dinosterol being derived from either dinoflagellates or diatoms, its presence throughout the sediment column indicates that the organisms were adapted to live in stratified water column conditions with fluctuating salinity in
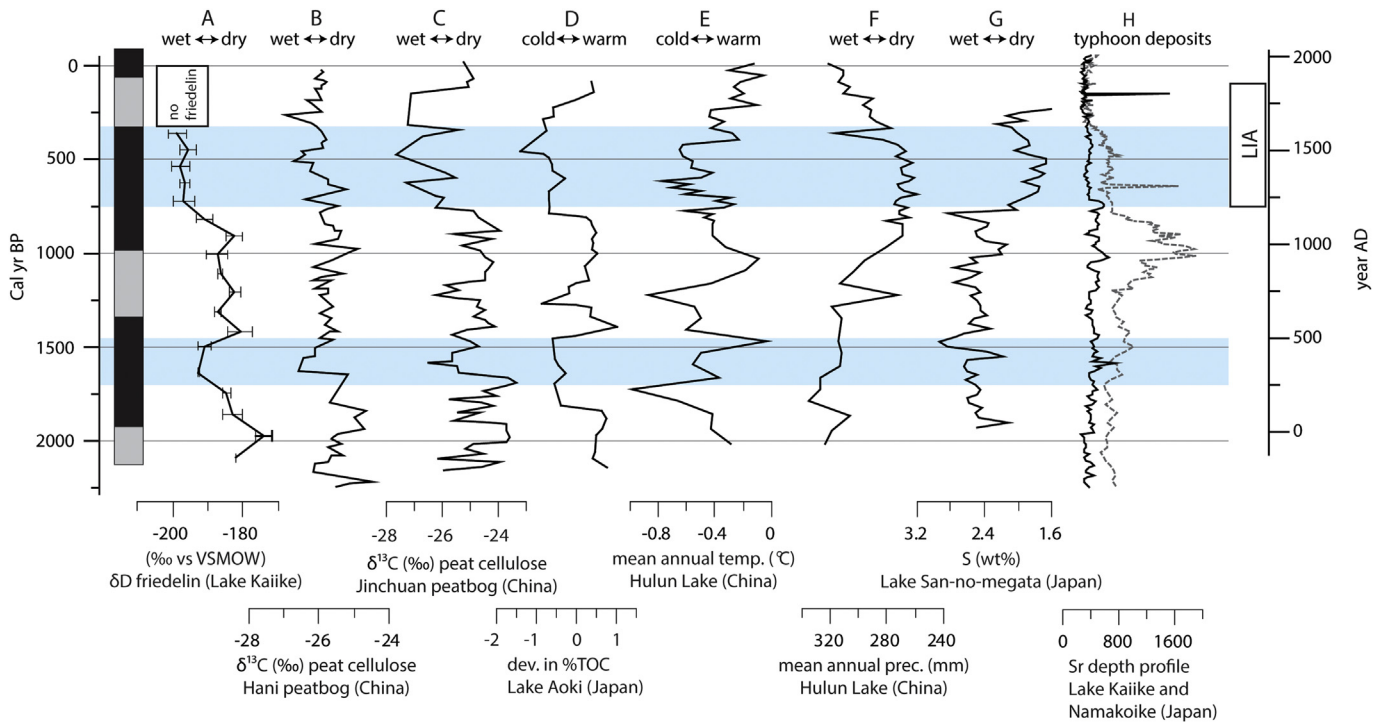
Figure 5. Comparison of Lake Kaiike (δD friedelin) and other regional records. (A) δD friedelin of Lake Kaiike (this study, error bars indicate the standard deviation based on duplicate measurements); δ13C records of peat cellulose (B) in the Hani peatbog (northern China) (Hong et al., 2005) and (C) in the Jinchuan peatbog (northern China) (Hong et al., 2001); (D) deviation in TOC contents (%) from a mean value of 5.8 in Lake Aoki, central Japan (Adhikari et al., 2002); (E) reconstructed temperatures, and (F) reconstructed precipitation from northeastern China after (Wen et al., 2010); (G) sulfur content (weight percentage) of sediments from Lake San-no-megata (northeastern Japan) (Yamada et al., 2010); (H) Sr abundance in Lake Kaiike and Lake Namakoike (Southwest Japan) (higher Sr abundances are indicative of marine inputs, indicating increased typhoon activity (Woodruff et al., 2009)). All locations can be found in Fig. 1. Blue horizontal bars indicate relatively wet intervals based on the hydrogen isotope record of Lake Kaiike. Panels (F) and (G) show opposite shifts in precipitation during the Little Ice Age (LIA) compared to panels (A), (B) and (C). The lithological column (left) shows dark, laminated, and organic-rich intervals (black) and bioturbated intervals with lower TOC content (gray). (For interpretation of the references to color in this figure legend, the reader is referred to the web version of this article.)

the surface waters. Although the TOC content is also reduced between 370 and 40 cal yr BP, tetrahymanol is also present in this interval, indicating that the lake was at least periodically stratified.

As there are no indications for substantial sea-level fluctuations over the past 2000 yr in this region (Nagaoka et al., 1996; Yokoyama et al., 1996), water column stratification/ventilation must have been related to other local environmental changes. Breaches in the gravel bar that separates the lake from the marine environment provide one explanation. Higher Sr concentrations in certain intervals in Lake Kaiike and the neighboring Lake Namakoike were previously interpreted by Woodruff et al. (2009) to represent past breaches in the gravel bar, allowing Sr-rich marine material to enter the lakes (Fig. 5H). These breaches could be the result of an increase in typhoon activity on Kamikoshiki Island (Woodruff et al., 2009). However, higher Sr concentrations at Lake Namakoike only partly coincide with the intervals characterized by low TOC contents, while at Lake Kaiike, there appears to be no or very little changes in Sr concentrations over the past 2000 yr (Woodruff et al., 2009). Perhaps higher Sr concentrations in the lake sediments do not (only) result from breaches in the barrier, but possibly also result from overwash of Sr-rich marine sediment (e.g., shell material) during typhoon landfall events. Since such a scenario does not require breaches in the gravel bar, the water column would have remained stratified following typhoon events. Moreover, the large amount of precipitation associated with typhoon landfall events might even have enhanced stratification rather than causing water column turnover. Similarly, periods of enhanced drought might have resulted in water column ventilation due to thinning of the fresh-water surface layer.

Past precipitation patterns

In the sediments of Lake Kaiike, *n*-alkane concentrations were relatively low, while friedelin was abundant in most of the sedimentary record. Therefore, hydrogen isotope ratios were determined for friedelin. Unlike *n*-alkanes, the relation between δD values of friedelin and rainwater has not been calibrated for present day conditions. However, friedelin is expected to derive from a similar higher terrestrial plant source (Chandler and Hooper, 1979), and therefore we assume a relation to precipitation isotope composition similar to that of *n*-alkanes. Hydrogen isotope ratios of modern precipitation are close to −30‰ during the winter months (December, January, and February), then gradually decrease and reach minimum values of around −60‰ during the peak of the summer monsoon in June and July (Fig. 4). Evapotranspiration leaves the water enriched in heavy isotopes relative to precipitation (Rozanski et al., 2001; Sachse et al., 2006). Biosynthetic fractionation accounts for the largest shift in the isotopic composition, and depletes the signal as recorded in the organic molecules (Sachse et al., 2004). Fractionation is also different for the different photosynthetic pathways (Bi et al., 2005; Liu et al., 2006; Sachse et al., 2012), and even under similar environmental conditions differences in fractionation may occur between different plants (Hou et al., 2007). Since the exact source of friedelin in the Lake Kaiike sediments is unknown, and little is known about the vegetation cover surrounding the lake, the observed changes in δD values may possibly be explained by changes in friedelin sources rather than changing precipitation patterns. Such a change in terrestrial higher plant cover in the surrounding of Lake Kaiike

would most likely also affect concentrations of leaf wax-derived lipids. Shifts in δD values of friedelin are, however, not accompanied by changes in the concentration of friedelin and/or long chain *n*-alkanes and *n*-alcohols, or in ACL and CPI (Fig. 3). Hence, rather than vegetation changes, the shifts in δD values most likely result from changes in δD values of source water, with more negative values corresponding to higher amounts of rainfall (Dansgaard, 1964).

A shift in friedelin δD values towards lower values after 1970 cal yr BP indicates a change from relatively dry to wetter conditions. Friedelin subsequently shows less negative values between 1420 and 910 cal yr BP, indicating reduced moisture, after which there is a shift to wetter conditions. Thus, the two intervals with enhanced water column ventilation, before 1970 cal yr BP and between 1310 and 1000 cal yr BP, occur during periods also characterized by relatively dry conditions. Decreased precipitation and consequently thinning of the fresh water surface layer may thus have facilitated water column ventilation.

Late Holocene climate in Northeast Asia

The precipitation reconstruction from Lake Kaiike shows two relatively wet phases (Fig. 5), the most recent of which coincides with the Little Ice Age, a pronounced cool phase that appears to have had its strongest impacts in the high northern latitudes (Mann et al., 2009), but also resulted in cooling across large parts of Asia (e.g., Adhikari et al., 2002; Wen et al., 2010). The atmospheric conditions during this cool phase resulted in an intensification of the hydrological cycle and increased precipitation rates in parts of China (e.g., Hong et al., 2001, 2005; Chen et al., 2006), as well as in Southwest Japan (this study).

Hong et al. (2005) found that changes in the intensity of the East Asian and Indian monsoon occur with an ENSO-like pattern, both on an orbital time scale and superimposed centennial to millennial scales. A link between ENSO and East Asian Summer Monsoon intensity can be explained by colder conditions in the west-central Pacific during El Niño events and the development of a high pressure cell (anticyclone) over this area during summer, which intensifies the monsoonal winds and hence moisture transport from the Pacific to the Asian continent (Wang et al., 2000). During the two phases of more intense rainfall in Southwest Japan during the late Holocene, climate in Northeast China was also more humid (Fig. 5B, C); Hong et al. (2005) linked these phases to the prevalence of El Niño-like conditions in the Pacific. Interestingly, precipitation reconstructions from further north in Japan (Yamada et al., 2010) and China (Wen et al., 2010) show opposite changes, with relatively dry conditions during the Little Ice Age (Fig. 5F, G). These contrasting rainfall patterns within a relatively small region (Japan and Northeast China) demonstrate the complexity of atmospheric circulation in this region, which is not only influenced by ENSO variability, but also by other atmospheric circulation patterns. For example the West Pacific Oscillation can cause local differences in precipitation patterns in northeast Asia (e.g., Aizen et al., 2001). High-resolution reconstructions of the hydrological cycle are needed to better constrain past changes in the East Asian monsoon in this highly dynamic area to predict how future climate change might affect local monsoon intensities.

Conclusions

A molecular δD record of sediments from Lake Kaiike shows two relatively wet intervals occurred during the past 2000 yr. The sediments of the lake alternate between laminated and bioturbated intervals. Anoxic bottom waters are caused by salinity stratification of the lake, due to a freshwater layer on top of saline deep waters.

Possibly, lower precipitation rates resulted in thinning of the freshwater surface layer and eventually in water column mixing. Our δD record shows that precipitation increased between 1640 and 1490 cal yr BP and between 720 and 370 yr BP, of which the last period corresponds with the Little Ice Age. These results are consistent with other climate reconstructions from China and Japan and likely result from El Niño-like oscillations in the coupled ocean−atmosphere system. The sensitivity of Northeast Asia to decadal to centennial-scale shifts in atmospheric circulation is confirmed when comparing the results from southwestern Japan with records from northeastern Japan and northeast China. Especially during the Little Ice Age, the northern part of Japan becomes drier while farther south the precipitation rates increase. Such regional differences can result from climate oscillations like the Western Pacific Oscillation. However, more high-resolution records of northwest Asia are needed to better understand the effect of climate oscillations and the East Asian Summer Monsoon on the different regions in this area.

References

Adhikari, D.P., Kumon, F., Kawajiri, K., 2002. Holocene climate variability as deduced from the organic carbon and diatom records in the sediments of Lake Aoki, central Japan. The Journal of the Geological Society of Japan 108, 249−265.

Aizen, E.M., Aizen, V.B., Melack, J.M., Nakamura, T., Ohta, T., 2001. Precipitation and atmospheric circulation patterns at mid-latitudes of Asia. International Journal of Climatology 21, 535−556. http://dx.doi.org/10.1002/joc.626.

Alam, M., Sansing, T.B., Busby, E.L., Martiniz, D.R., Ray, S.M., 1979. Dinoflagellate sterols I: sterol composition of the dinoflagellates of *Gonyaulax* species. Steroids 33, 197−203.

Bi, X., Sheng, G., Liu, X., Li, C., Fu, J., 2005. Molecular and carbon and hydrogen isotopic composition of *n*-alkanes in plant leaf waxes. Organic Geochemistry 36, 1405−1417. http://dx.doi.org/10.1016/j.orggeochem.2005.06.001.

Boon, J.J., Rijpstra, W.I.C., De Lange, F., De Leeuw, J.W., Yoshioka, M., Shimizu, Y., 1979. Black Sea sterol-a molecular fossil for dinoflagellate blooms. Nature 277, 125−127.

Chandler, R.F., Hooper, S.N., 1979. Friedelin and associated triterpenoids. Phytochemistry 18, 711−724.

Chang, C.-P., Zhang, Y., Li, T., 2000. Interannual and interdecadal variations of the East Asian summer monsoon and tropical Pacific SSTs. Part I: roles of the subtropical ridge. Journal of Climate 13, 4310−4325.

Chen, F., Huang, X., Zhang, J., Holmes, J.A., Chen, J., 2006. Humid Little Ice Age in arid central Asia documented by Bosten Lake, Xinjiang, China. Science in China Series D: Earth Sciences 49, 1280−1290.

Chikaraishi, Y., Kaneko, M., Ohkouchi, N., 2012. Stable hydrogen and carbon isotopic compositions of long-chain (C_{21}–C_{33}) *n*-alkanes and *n*-alkenes in insects. Geochimica et Cosmochimica Acta 95, 53−62.

Dansgaard, W., 1964. Stable isotopes in precipitation. Tellus 16, 436−468.

Eglinton, G., Hamilton, R.J., 1967. Leaf epicuticular waxes. Science 156, 1322−1335.

Elsner, J.B., Liu, K.B., 2003. Examining the ENSO-typhoon hypothesis. Climate Research 25, 43−54.

Gong, D.-Y., Ho, C.-H., 2003. Arctic oscillation signals in the East Asian summer monsoon. Journal of Geophysical Research: Atmospheres 108, 4066.

Hong, Y.T., Hong, B., Lin, Q.H., Shibata, Y., Hirota, M., Zhu, Y.X., Leng, X.T., Wang, Y., Wang, H., Yi, L., 2005. Inverse phase oscillations between the East Asian and Indian Ocean summer monsoons during the last 12 000 years and paleo-El Niño. Earth and Planetary Science Letters 231, 337−346.

Hong, Y.T., Wang, Z.G., Jiang, H.B., Lin, Q.H., Hong, B., Zhu, Y.X., Wang, Y., Xu, L.S., Leng, X.T., Li, H.D., 2001. A 6000-year record of changes in drought and precipitation in northeastern China based on a $\delta^{13}C$ time series from peat cellulose. Earth and Planetary Science Letters 185, 111−119.

Hou, J., D'Andrea, W.J., MacDonald, D., Huang, Y., 2007. Hydrogen isotopic variability in leaf waxes among terrestrial and aquatic plants around Blood Pond, Massachusetts (USA). Organic Geochemistry 38, 977−984.

IAEA/WMO, 2016. Global Network of Isotopes in Precipitation. The GNIP Database. Accessible at: http://www.iaea.org/water.

Kotani, T., Ozaki, M., Matsuoka, K., Snell, T.W., Hagiwara, A., 2001. Reproductive isolation among geographically and temporally isolated marine Brachionus strains. Hydrobiologia 446–447, 283–290.

Lau, K.-M., Li, M.-T., 1984. The monsoon of East Asia and its global associations - a survey. Bulletin of the American Meteorological Society 65, 114–125.

Lawrimore, J.H., Menne, M.J., Gleason, B.E., Williams, C.N., Wuertz, D.B., Vose, R.S., Rennie, J., 2011. An overview of the Global Historical Climatology Network monthly mean temperature data set, version 3. Journal of Geophysical Research 116, D19121. http://dx.doi.org/10.1029/2011JD016187.

Lim, J., Matsumoto, E., Kitagawa, H., 2005. Eolian quartz flux variations in Cheju Island, Korea, during the last 6500 yr and a possible Sun–monsoon linkage. Quaternary Research 64, 12–20.

Liu, W., Yang, H., 2008. Multiple controls for the variability of hydrogen isotopic compositions in higher plant *n*-alkanes from modern ecosystems. Global Change Biology 14, 2166–2177.

Liu, W., Yang, H., Li, L., 2006. Hydrogen isotopic compositions of *n*-alkanes from terrestrial plants correlate with their ecological life forms. Oecologia 150, 330–338.

Lopez, J.F., de Oteyza, T.G., Teixidor, P., Grimalt, J.O., 2005. Long chain alkenones in hypersaline and marine coastal microbial mats. Organic Geochemistry 36, 861–872.

Mann, M.E., Zhang, Z., Rutherford, S., Bradley, R.S., Hughes, M.K., Shindell, D., Ammann, C., Faluvegi, G., Ni, F., 2009. Global signatures and dynamical origins of the Little Ice Age and Medieval Climate Anomaly. Science 326, 1256–1260.

Marlowe, I.T., Brassell, S.C., Eglinton, G., Green, J.C., 1990. Long-chain alkenones and alkyl alkenoates and the fossil coccolith record of marine sediments. Chemical Geology 88, 349–375.

Marlowe, I.T., Green, J.C., Neal, A.C., Brassell, S.C., Eglinton, G., Course, P.A., 1984. Long chain (n-C$_{37}$–C$_{39}$) alkenones in the Prymnesiophyceae. Distribution of alkenones and other lipids and their taxonomic significance. British Phycological Journal 19, 203–216.

Matsuyama, M., 1977. Limnological features of Lake Kaiike, a small coastal lake on Kamikoshiki Island, Kagoshima Prefecture, Japan. Japanese Journal of Limnology 38, 9–18.

Nagaoka, S., Yokoyama, Y., Nakada, M., Maeda, Y., 1996. Holocene sea-level change in the Goto Islands, Japan. Geographical Reports of Tokyo Metropolitan University 31, 11–18.

Nakajima, Y., Okada, H., Oguri, K., Suga, H., Kitazato, H., Koizumi, Y., Fukui, M., Ohkouchi, N., 2003. Distribution of chloropigments in suspended particulate matter and benthic microbial mat of a meromictic lake, Lake Kaiike, Japan. Environmental Microbiology 5, 1103–1110.

Rontani, J.-F., Beker, B., Volkman, J.K., 2004. Long-chain alkenones and related compounds in the benthic haptophyte *Chrysotila lamellosa* Anand HAP 17. Phytochemistry 65, 117–126.

Rozanski, Kazimer, Froehlich, Klaus, Mook, Willem G., 2001. Environmental Isotopes in the Hydrological Cycle: Principals and Applications. In: Technical Documents in Hydrology. IAEA and UNESCO, Paris.

Sachse, D., Billault, I., Bowen, G.J., Chikaraishi, Y., Dawson, T.E., Feakins, S.J., Freeman, K.H., Magill, C.R., McInerney, F.A., van der Meer, M.T.J., Polissar, P., Robins, R.J., Sachs, J.P., Schmidt, H.-L., Sessions, A.L., White, J.W.C., West, J.B., Kahmen, A., 2012. Molecular paleohydrology: interpreting the hydrogen-isotopic composition of lipid biomarkers from photosynthesizing organisms. Annual Review of Earth and Planetary Sciences 40, 221–249.

Sachse, D., Radke, J., Gleixner, G., 2006. δD values of individual *n*-alkanes from terrestrial plants along a climatic gradient – implications for the sedimentary biomarker record. Organic Geochemistry 37, 469–483.

Sachse, D., Radke, J., Gleixner, G., 2004. Hydrogen isotope ratios of recent lacustrine sedimentary *n*-alkanes record modern climate variability. Geochimica et Cosmochimica Acta 68, 4877–4889.

Sainsbury, M., 1970. Friedelin and epifriedelinol from the bark of Prunus turfosa and a review of their natural distribution. Phytochemistry 9, 2209–2215.

Sinninghe Damsté, J.S., Kenig, F., Koopmans, M.P., Köster, J., Schouten, S., Hayes, J.M., de Leeuw, J.W., 1995. Evidence for gammacerane as an indicator of water column stratification. Geochimica et Cosmochimica Acta 59, 1895–1900.

Stuiver, M., Reimer, P.J., Reimer, R., 2015. Calib Radiocarbon Calibration.

Takishita, K., Chikaraishi, Y., Leger, M.M., Kim, E., Yabuki, A., Ohkouchi, N., Roger, A.J., 2012. Lateral transfer of tetrahymanol-synthesizing genes has allowed multiple diverse eukaryote lineages to independently adapt to environments without oxygen. Biology Direct 7, 5.

Volkman, J.K., 2005. Sterols and other triterpenoids: source specificity and evolution of biosynthetic pathways. Organic Geochemistry 36, 139–159.

Volkman, J.K., Barrett, S.M., Dunstan, G.A., Jeffrey, S.W., 1993. Geochemical significance of the occurrence of dinosterol and other 4-methyl sterols in a marine diatom. Organic Geochemistry 20, 7–15.

Volkman, J.K., Eglinton, G., Corner, E.D.S., Forsberg, T.E.V., 1980. Long-chain alkenes and alkenones in the marine coccolithophorid *Emiliania huxleyi*. Phytochemistry 19, 2619–2622.

Wang, B., Chan, J.C.L., 2002. How strong ENSO events affect tropical storm activity over the western North Pacific. Journal of Climate 15, 1643–1658.

Wang, B., Lin, H., 2002. Rainy season of the Asian–Pacific summer monsoon. Journal of Climate 15, 386–398.

Wang, B., Wu, R., Fu, X., 2000. Pacific–East Asian teleconnection: how does ENSO affect East Asian climate? Journal of Climate 13, 1517–1536.

Wang, Y.J., Cheng, H., Edwards, R.L., An, Z.S., Wu, J.Y., Shen, C.-C., Dorale, J.A., 2001. A high-resolution absolute-dated late Pleistocene monsoon record from Hulu Cave, China. Science 294, 2345–2348.

Wen, R., Xiao, J., Chang, Z., Zhai, D., Xu, Q., Li, Y., Itoh, S., 2010. Holocene precipitation and temperature variations in the East Asian monsoonal margin from pollen data from Hulun Lake in northeastern Inner Mongolia, China. Boreas 39, 262–272.

Woodruff, J.D., Donnelly, J.P., Okusu, A., 2009. Exploring typhoon variability over the mid-to-late Holocene: evidence of extreme coastal flooding from Kamikoshiki, Japan. Quaternary Science Reviews, Quaternary Ice Sheet-Ocean Interactions and Landscape Responses 28, 1774–1785.

Wu, R., Wang, B., 2002. A contrast of the East Asian summer monsoon–ENSO relationship between 1962–77 and 1978–93. Journal of Climate 15, 3266–3279.

Yamada, K., Kamite, M., Saito-Kato, M., Okuno, M., Shinozuka, Y., Yasuda, Y., 2010. Late Holocene monsoonal-climate change inferred from Lakes Ni-no-Megata and San-no-Megata, northeastern Japan. Quaternary International, Climate Dynamics and Prehistoric Occupation: Eurasian Perspectives on Environmental Archaeology 220, 122–132.

Yamaguchi, K.E., Oguri, K., Ogawa, N.O., Sakai, S., Hirano, S., Kitazato, H., Ohkouchi, N., 2010. Geochemistry of modern carbonaceous sediments overlain by a water mass showing photic zone anoxia in the saline meromictic Lake Kaiike, southwest Japan: I. Early diagenesis of organic carbon, nitrogen, and phosphorus. Palaeogeography, Palaeoclimatology, Palaeoecology 294, 72–82.

Yanai, M., Li, C., Song, Z., 1992. Seasonal heating of the Tibetan Plateau and its effects on the evolution of the Asian summer monsoon. Journal of the Meteorological Society of Japan 70, 319–351.

Yihui, D., Chan, J.C.L., 2005. The East Asian summer monsoon: an overview. Meteorology and Atmospheric Physics 89, 117–142.

Yokoyama, Y., Nakada, M., Maeda, Y., Nagaoka, S., Okuno, J., Matsumoto, E., Sato, H., Matsushima, Y., 1996. Holocene sea-level change and hydro-isostasy along the west coast of Kyushu, Japan. Palaeogeography, Palaeoclimatology, Palaeoecology 123, 29–47.

Yokoyama, Y., Naruse, T., Ogawa, N.O., Tada, R., Kitazato, H., Ohkouchi, N., 2006. Dust influx reconstruction during the last 26,000 years inferred from a sedimentary leaf wax record from the Japan Sea. Global and Planetary Change 54, 239–250.

Zink, K.-G., Leythaeuser, D., Melkonian, M., Schwark, L., 2001. Temperature dependency of long-chain alkenone distributions in recent to fossil limnic sediments and in lake waters. Geochimica et Cosmochimica Acta 65, 253–265.